Chemical tools to modulate endocannabinoid biosynthesis

Deng, H.

4

Diacylglycerol lipase inhibitors prevent fasting-induced refeeding in mice

Based on
H. Deng, S. Kooijman, A. M.C.H. van den Nieuwendijk, D. Ogasawara, T. van der Wel, F. van Dalen, M. P. Baggelaar, F. J. Janssen, R. J.B.H.N. van den Berg, H. den Dulk, K. Vasu, H. Thomas, B. F. Cravatt, H. S. Overkleeft, P. C.N. Rensen, M. van der Stelt, *J. Med. Chem.*

Introduction

Activation of the cannabinoid CB_1 receptor is a clinically proven signalling pathway controlling the energy balance in humans.[1] Rimonabant, a cannabinoid CB_1 receptor inverse agonist, reduced body weight and waist circumference in obese patients and improved cardiovascular risk factors, possibly via reducing food intake and increasing energy expenditure through activation of thermogenic brown adipose tissue.[2] First, several lines of evidence suggest that the endocannabinoid 2-arachidonoylglycerol (2-AG) regulates cannabinoid CB_1 receptor-dependent food intake. Second, 2-AG levels are increased in the hypothalamus of fasting mice and pharmacological intervention using the non-selective fluorophosphonate-based diacylglycerol lipase (DAGL) inhibitors O-5596 and O-7460 lead to reduced food intake in mice.[3,4] Third, DAGLα$^{-/-}$ mice showed hypophagia and leanness similar to that of $CB_1^{-/-}$ mice, while knockout mice of DAGLβ and *N*-acyl phosphatidylethanolamine phospholipase D (NAPE-PLD, the main enzyme responsible for anandamide biosynthesis) did not share this phenotype.[5,6] Interestingly, DAGLα knockout mice also had low fasting insulin, triglyceride, and total cholesterol

levels, and after glucose challenge had normal glucose, but very low insulin levels.[6] Fourth, mice overexpressing monoacylglycerol lipase, the enzyme that inactivates 2-AG, were lean, hyperphagic, resistant to diet induced obesity, hyperthermic and hypersensitive to β_3-adrenergic-stimulated thermogenesis.[7] Taken together, these data suggest that selective interference with DAGLα signaling may represent a novel therapeutic avenue to treat obesity and the metabolic syndrome.

In Chapters 2 and 3, the development and characterization of brain active DAGL inhibitors DH376 and DO34 was described. Competitive ABPP studies revealed a complementary selectivity profile for DH376 and DO34. Administration of DH376 and DO34 to mice significantly decreased 2-AG levels in the brain in a time- and dose dependent manner[8]. In this Chapter, the therapeutic efficacy of DH376 and DO34 as a potential anti-obesity agents is explored by studying their effect on fasting-induced food intake in mice, which is a typical cannabinoid CB_1 receptor mediated behavior.

Results and discussion

In vivo efficacy of DH376 and DO34

Mice were fasted for 18h and received a single intraperitoneal injection of vehicle or DH376 (50 mg/kg) 30 min before refeeding, and cumulative food intake was measured up to 16h. Within 2h, DH376-treated mice only consumed a third of the food compared to the vehicle-treated mice, and the effect of reduction in food-take maintained up to 4h (Figure 1a-d). After 16h, however, food intake in DH376-treated mice was back to the same levels as in vehicle-treated mice (Figure 1d), which paralleled the recovery of brain 2-AG levels. Consistent with the delay in refeeding of DH376-treated mice, indirect calorimetric measurements indicated that carbohydrate and fat oxidation remained respectively low and high for a prolonged period (Figure 1e,f). Importantly, DH376-treated mice showed no effect on locomotor activity (Figure 1g, over 4h; Figure 1h, over 24h) as measured by infrared beam breaks in Y and Z planes. Altogether, these results support the notion that DAGLα regulates food intake.

In Chapter 3, another CNS-active DAGL inhibitor (DO34) and a structurally related control probe DO53 were reported. DO34 reduced brain 2-AG levels in dose- and time-dependent manner, whereas the control probe DO53 did not affect brain 2-AG levels. Therefore, the effects of DO34 and DO53 were examined on fasting-induced refeeding, indirect calorimetry and locomotor activity. It was observed that food intake was completely blocked in DO34-treated mice, which was again also reflected by the calorimetric measurements. Surprisingly, control probe DO53-treated mice also showed significant reductions in fasting-induced refeeding, and both DO34- and DO53-treated mice were hypolocomotive (Figure 1g, h). These data suggest that there are one or more off-targets shared by the DAGL inhibitors and control probe DO53, that may also be involved in controlling food intake in fasting-induced mice. For

example, carboxylesterase was identified by *ex vivo* competitive ABPP in mouse liver as a major off-target shared by all three compounds (Figure 2).

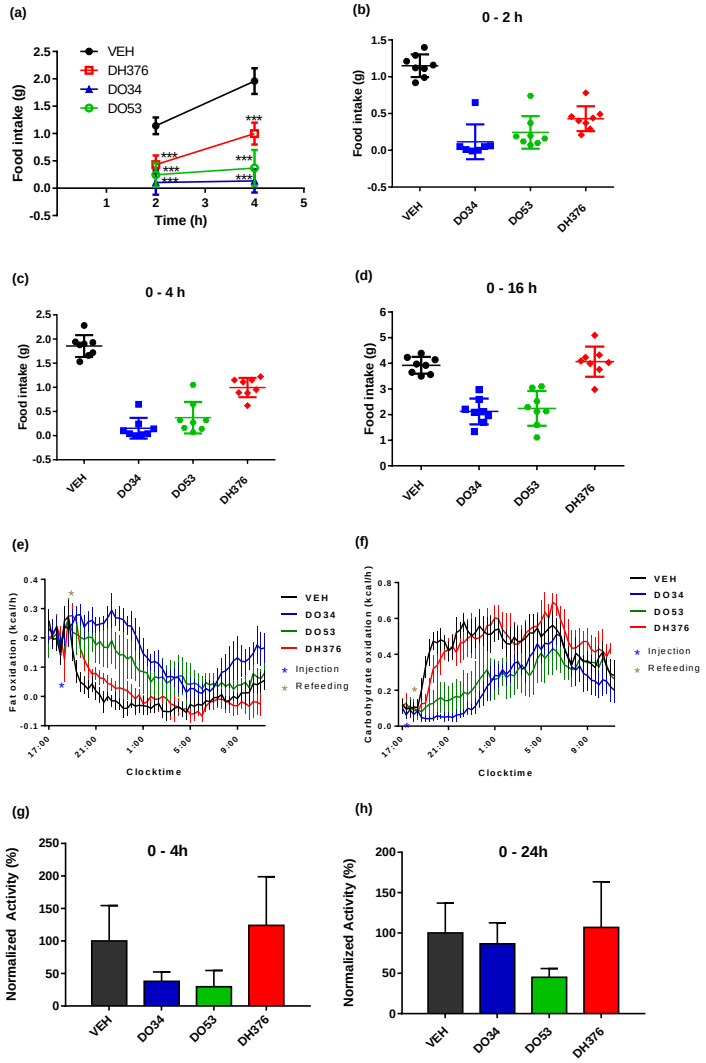

Figure 1. (a-h) *In vivo* effects of DAGL inhibitors DH376, DO34 and control compound DO53 on food intake (a-d), fat/carbohydrate oxidation (e, f) and locomotor activity (g, 0-4h; h, 0-24h) in mice. Cumulative food intake was measured in 18h fasted mice. The animals received a single intraperitoneal injection of vehicle (black), or DH376 (red), DO34 (blue), and DO53 (green) (50 mg/kg) 30 min before the start of refeeding and the testing period. The fat and carbohydrate oxidation of the animals were calculated from the $V{\cdot}O_2$ and $V{\cdot}CO_2$ in metabolic cages (in 20 min bins), and the locomotor activity over 4h of the animals was measured by infrared beam breaks in Y and Z axis. Data represent average values ± SEM; n = 8 mice per group.

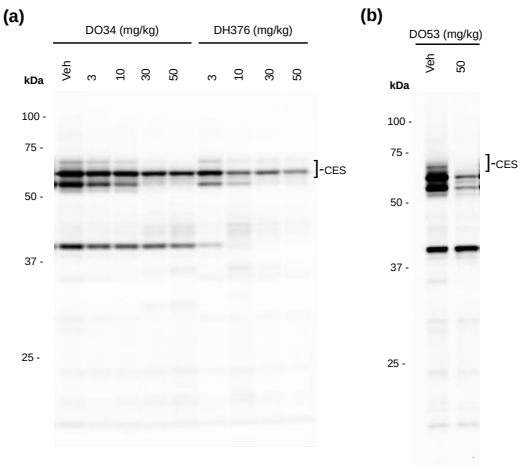

Figure 2. *Ex vivo* selectivity profile of DAGLs inhibitors (DH376 and DO34) and control compound (DO53) in mouse liver. (a) Competitive ABPP analysis in mouse liver from mice treated with various dose (3-20-30-50 mg/kg, i.p., 4h) of DAGLs inhibitors DH376 and DO34 using FP-TAMRA (1 µM, 20 min) as a broad-spectrum probe. (b) Competitive ABPP analysis in mouse liver from DO53-treated mice (50 mg/kg, i.p., 4h) using FP-TAMRA (1 µM, 20 min) as a probe.

A comprehensive profile of endogenous DAGLs activity in mouse tissues

DAGLs are not only expressed in the brain: their mRNA has also been found in peripheral tissues.[9] Genetic studies with constitutive knockout mice have revealed that DAGLα and DAGLβ regulate 2-AG production in a tissue-type dependent manner,[10-12] which may suggest that peripheral DAGLs also contribute to the control of energy balance.[13,14] Competitive activity-based protein profiling (ABPP) using the ABPs DH379 and MB064 was applied to investigate the role of endogenous DAGLα and DAGLβ activity in peripheral tissues, such as liver, kidney, spleen, heart, testis, lung, pancreas and muscle (Chapter 3).[8,15] DAGL inhibitors LEI105[16] and KT109[17] were applied to confirm the identity of the fluorescent bands. A fluorescent band at the molecular weight of DAGLα activity, which was out-competed with LEI105 and KT109, was detected in the brain proteomes treated with both probes, but not in other tissues (Figure 3). This is in line with previous ABPP results.[16] It is currently unknown why DAGLα activity can not be detected by ABPP in peripheral tissues, while mRNA and lipidomics studies indicate otherwise.[18] DH379 labeled a protein at the expected molecular weight of DAGLβ (using mouse brain as a reference) in spleen, kidney, testis, muscle, heart and lung. This labelling was prevented by pre-incubation with LEI105 and KT109 (1 µM, 30min) (Figure 3). Multiple fluorescent signals around ~70kDa were found in the liver, which make it difficult to unequivocally establish the

identity of DAGLβ in this tissue (Figure 3f). DH379 and MB064 can also label α,β-hydrolase domain containing protein 6 (ABHD6),[8, 19] an enzyme involved in lipid metabolism.[20,21] Strong ABHD6 labeling by both probes was observed in testis, liver and brain, whereas only a weak fluorescent band was detected in MB064-treated proteomes of the spleen, kidney, muscle and heart (Figure 3). (Of note, DH379 is less sensitive towards ABHD6.) Taken together, these data suggest that DAGLβ and ABHD6, rather than DAGLα, could be considered to play a peripheral role in controlling the energy balance.

A tissue-wide selectivity profile of DH376

Next, the *in vivo* target engagement and selectivity profile of DH376 was studied in various tissues from mice treated with a low or high dose of DH376 (3 and 30 mg/kg, respectively). Mice were sacrificed 2h after intraperitoneal administration and eight tissues (liver, kidney, spleen, heart, testis, lung, muscle and pancreas) were collected and analyzed by competitive ABPP using TAMRA-FP, a broad-spectrum serine hydrolase probe. Competitive ABPP revealed that DH376 maintained good selectivity for the DAGLβ in most tissues, particularly at the low dose (Figure 4a), whereas at the high dose various off-targets with a MW around 50-70 kDa were identified (Figure 4a). The identity of these off-targets is currently unknown, but carboxylesterases are potential candidates as was previously observed in mouse brain (Chapter 3).

Direct target engagement of DH376 in the mouse tissue proteomes was visualized by conjugation of probe-labeled proteins to a Cy5 fluorophore by copper-catalyzed azide-alkyne cycloaddition (CuAAC).[23] Consistent with the competitive ABPP results, direct conjugation revealed several off-targets at around ~65 kDa and 55 kDa (Figure 4b). In addition, a protein was labeled around 35 kDa, matching the molecular weight of ABHD6. Of note, the identified target band at ~70 kDa by CuAAC could be DAGLβ, but needs further confirmation with MS-based ABPP. Taken together, these results indicate that DH376 maintains relatively good selectivity in most of tissues; only in the liver DH376 cross-reacts with multiple off-targets.

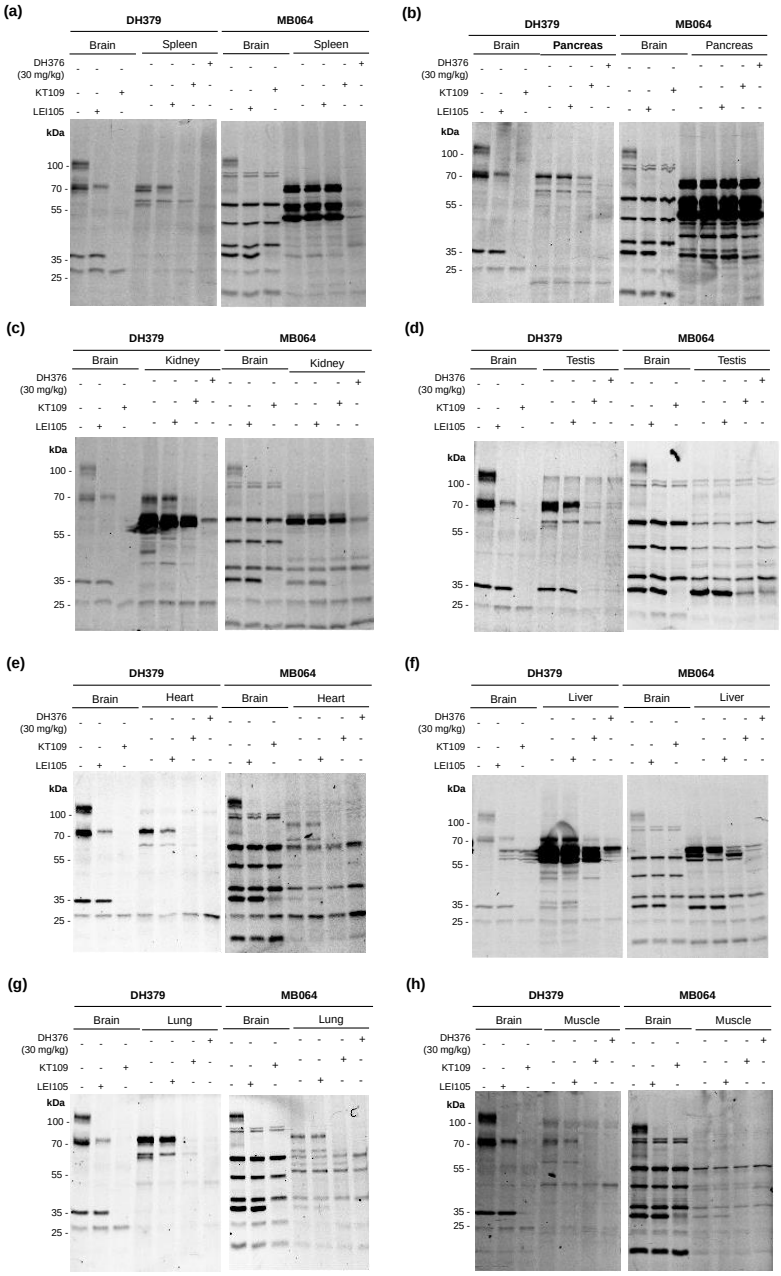

Figure 3. (a-h) Competitive ABPP was employed to screen a set of mouse tissues, including spleen (a), pancreas (b), kidney (c), testis (d), heart (e), liver (f), lung (g) and muscle (h) using DH379 and MB064 as ABPs and obtained a tissue-wide overview of endogenous activities of DAGLα, DAGLβ and ABHD6. Mouse membrane proteome was incubated at r.t. with vehicle (DMSO), LEI105 (1 μM)or KT109 (1μM) for 30 mins.

The sample was subsequently treated with MB064 (0.25 µM), or DH379 (1 µM) for 20 mins at r.t. DH376 (30 mg/kg)-treated mouse membranes as an *ex vivo* control were directly treated with MB064 (0.25 µM), or DH379 (1 µM) for 20 mins at r.t. The fluorescent bands at the molecular weight of ~120 kDa, 70 kDa or 35 kDa, which were prevented by pre-incubation of KT109 or LEI105, are DAGLα, DAGLβ and ABHD6, respectively. Of note, mouse brain was used as a reference for the detection of DAGLs and ABHD6 activity in other mouse tissues.

Table 1. Summary of detection endogenous DAGLα, DAGLβ and ABHD6 activity in mouse tissues using gel-based activity-based protein profiling (related to data from Figure 3).

	Brain	Spleen	Kidney	Testis	Heart	Lung	Liver	Muscle
DAGLα	+	-	-	-	-	-	-	-
DAGLβ	+	+	+	+	+	+	+	+
ABHD6	+	+	+	+	-	-	+	+

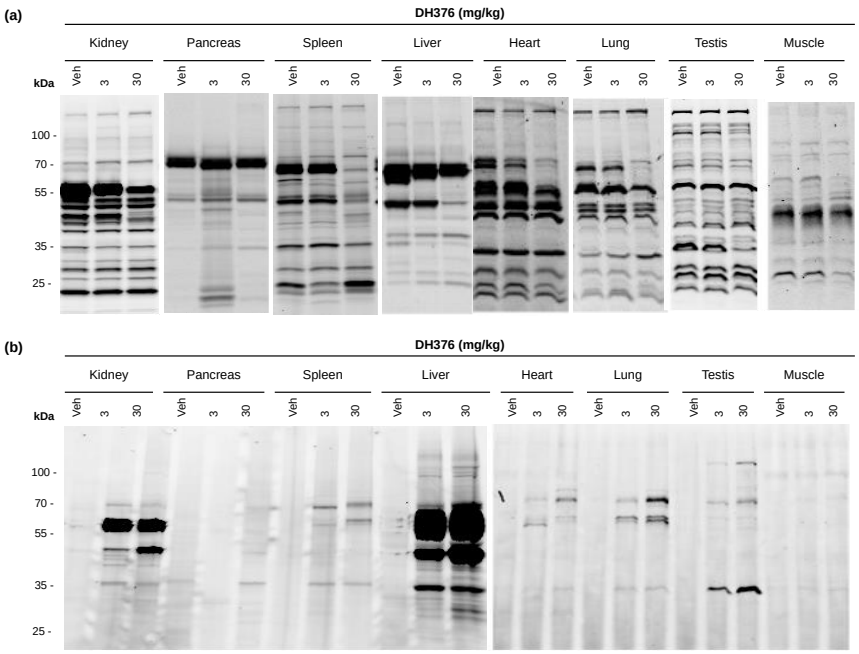

Figure 4. Gel-based ABPP analysis of various mouse tissue proteomes from mice treated with DH376 (3 or 30 mg/kg, i.p., 2h). (a) Competitive ABPP using a broad-spectrum probe TAMRA-FP to measure selectivity profile of DH376 over serine hydrolases. Tissue membrane proteomes from DH376-treated mice were incubated with TAMRA-FP (0.5 µM, 20 min) at r.t. (b) Click chemistry (CuAAC) ABPP of tissues membranes from DH376-treated mice. Tissue membrane proteomes were conjugated with Cy5-azide for 1h followed by SDS-PAGE and in-gel fluorescence scanning. The protein bands (off-targets) were directly visualized.

Conclusions

In summary, *in vivo* efficacy of CNS-active DAGLs inhibitors (DH376 and DO34) was demonstrated in a mouse model of fasting-induced refeeding, which is a typical cannabinoid CB_1-receptor-mediated response. These effects are in line with the phenotypes observed with DAGLα and CB_1 receptor knockout mice. The results also stress the importance of using a negative control compound, because DO53 also reduced food intake and affected locomotion, which indicates that triazole urea inhibitors affect the energy balance and locomotion in mice through multiple, yet to be discovered, molecular targets. While DH376 was found to maintain good selectivity in most of tissues, some other off-targets were also observed. This comprehensive tissue-wide detection of DAGL activity may provide important information for the design of future studies to investigate the peripheral role of DAGLs.

Experimental section

Materials of chemical biological assays

MB064 and DH379 were synthesized according to a previously described protocol.[24-28] FP-TAMRA is commercially available at Thermo Fischer Scientific.

ABPP enzyme activity measurements

The percentage of activity was determined by measuring the integrated optical intensity of the fluorescent protein bands using image lab 4.1. The relative intensity was compared to the vehicle treated proteins, the strongest signal set to 100% after protein loading correction using Coomassie Blue gel. Enzyme activity figures were generated using GraphPad Prism software 7.0.

Preparation of tissue proteomes

Mouse tissues were dounce homogenized in lysis buffer (20 mM HEPES, 250 mM sucrose, 2 mM DTT, 1 mM $MgCl_2$ with or without 25 U/mL benzonase) and incubated in ice for 5 min, followed by a low-speed spin (1,400−2,500 x g, 3 min, 4 °C) to remove debris. The membrane and cytosolic fractions were separated by ultracentrifugation (100,000 x g, 45 min, 4 °C) of the resulting homogenate lysate. After removal of the soluble supernatant, the membrane pellet was washed 1X with cold HEPES buffer (20 mM, with or without 2 mM DTT) followed by resuspension in cold HEPES buffer (20 mM, with or without 2 mM DTT) by pipetting. Total protein concentrations in membrane and soluble fractions were determined using the Bio-Rad DC protein assay kit. Samples were stored at -80 °C until further use.

Tissue profiling by gel-based competitive ABPP

Gel-based ABPP assays were performed as previously reported.[29] Cell or tissue proteomes were treated with either FP-TAMRA (1 µM or 500 nM final concentration), MB064 (0.25 µM final concentration), or DH379 (1 µM final concentration). For MB064 and DH379 labeled samples, 2 mg/mL of proteome was used to enhance endogenous DAGL signals; 1 mg/mL proteome was used for labeling with FP-TAMRA. Probe labeling was carried out for 30 min at r.t., followed by addition of 4X SDS-PAGE loading buffer to quench the reaction. After separation by SDS-PAGE (10% acrylamide), samples were visualized by in-gel fluorescence scanning using a ChemiDoc MP system.

Copper-catalyzed azide-alkyne cycloaddition (CuAAC or click) chemistry-ABPP

Mouse brain membrane proteomes from either naïve (*in vitro*) or inhibitor-treated (*in vivo*) mice were prepared for analysis as described in preparation of tissue proteome. Using previously developed methods[30], Cyanine 5-Azide (Cy5−N_3) was conjugated to each alkyne probe for in-gel analysis. Briefly, $CuSO_4$ (1.0 µL/reaction, 100 mM in H_2O), THPTA (0.2 µL/reaction, 100 mM in H_2O), sodium ascorbate (0.6 µL/reaction, 1 M in H_2O [freshly prepared]), and Cy5−N_3 (0.2 µL/reaction, 0.4 mM in DMSO) were premixed. This click reagent mixture (2.0 µL total volume) was immediately added to each proteome (18 µL), and the reaction was stirred by briefly vortexing. After 1 h at room temperature, reactions were diluted with 4× SDS loading buffer (10 µL) and resolved by SDS-PAGE.

***In vivo* target engagement studies of DH376**

The animal experiments were conducted in accordance with the ethical committee of Leiden University (DEC#14137). *In vivo* studies with DH376 were conducted in C57BL/6 mice. Mice were injected with DH376 (3 or 30 mg/kg) i.p. in 18:1:1 (v/v/v) solution of saline/ethanol/PEG40 (ethoxylated castor oil, 10 µL/g body weight of mouse). After 2h, mice were anesthetized with isoflurane, and euthanized by cervical dislocation. Mice were perfused with PBS and then brain, liver, spleen, heart, lung, pancreas, testis, muscle and kidney were collected. Tissue homogenates were prepared and competitive ABPP experiments were performed according to the previously described method.[8]

***In vivo* food intake studies with DH376, DO34 and DO53**

All animal experiments were approved by the Ethics Committee on Animal Care and Experimentation of the Leiden University Medical Center. 12-week-old male C57Bl/6J mice (Charles River, Saint-Germain-Nuelles, France) were single housed in metabolic cages (LabMaster System, TSE Systems, Bad Homburg, Germany) with a regular 12:12h light/dark cycle (6 a.m.- 6 p.m.) and free access to food and water unless noted otherwise. After 3 days of acclimatization, mice were fasted for 18h starting at midnight followed by an intraperitoneal injection with DH376 (50 mg/kg), DO34 (50

mg/kg), DO53 (50 mg/kg) or vehicle 30 min prior to refeeding. Solutions were prepared in mixture of saline/ethanol/PEG40 (18:1:1; v/v/v). Cumulative food intake, oxygen uptake ($V{\cdot}O_2$), carbon dioxide production ($V{\cdot}CO_2$) and physical activity (beam breaks) were monitored. Carbohydrate oxidation was calculated using the formula ((4.585* $V{\cdot}CO_2$)-(3.226* $V{\cdot}O_2$))*4, in which the 4 represents the conversion from mass per time unit to kcal per time unit. Similarly, fat oxidation was calculated using the formula ((1.695* $V{\cdot}O_2$)-(1.701* $V{\cdot}CO_2$))*9.

Supporting Figures

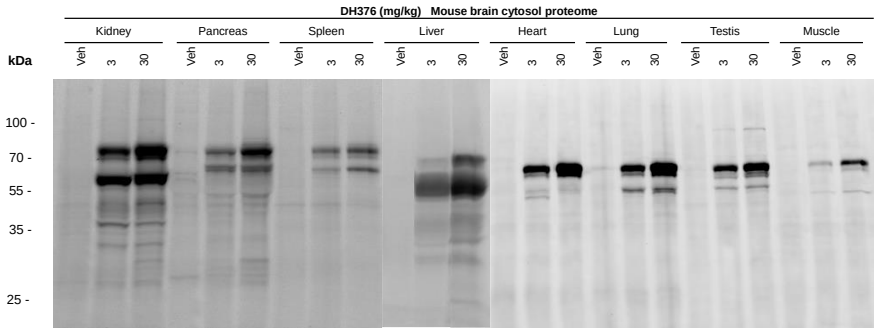

Figure S.1. Click chemistry (CuAAC) ABPP of tissue cytosols from DH376-treated mice. Tissue cytosol proteomes were conjugated with Cy5-azide for 1h followed by SDS-PAGE and in-gel fluorescence scanning. The protein bands (off-targets) in cytosol were directly visualized.

References

1. Di Marzo, V.; Matias, I. Endocannabinoid control of food intake and energy balance. *Nature Neuroscience* **2005,** 8, 585-589.
2. Boon, M. R.; Kooijman, S.; van Dam, A. D.; Pelgrom, L. R.; Berbee, J. F. P.; Visseren, C. A. R.; van Aggele, R. C.; van den Hoek, A. M.; Sips, H. C. M.; Lombes, M.; Havekes, L. M.; Tamsma, J. T.; Guigas, B.; Meijer, O. C.; Jukema, J. W.; Rensen, P. C. N. Peripheral cannabinoid 1 receptor blockade activates brown adipose tissue and diminishes dyslipidemia and obesity. *FASEB Journal* **2014,** 28, 5361-5375.
3. Bisogno, T.; Mahadevan, A.; Coccurello, R.; Chang, J. W.; Allara, M.; Chen, Y. G.; Giacovazzo, G.; Lichtman, A.; Cravatt, B.; Moles, A.; Di Marzo, V. A novel fluorophosphonate inhibitor of the biosynthesis of the endocannabinoid 2-arachidonoylglycerol with potential anti-obesity effects. *British Journal of Pharmacology* **2013,** 169, 784-793.
4. Janssen, F. J.; van der Stelt, M. Inhibitors of diacylglycerol lipases in neurodegenerative and metabolic disorders. *Bioorganic & Medicinal Chemistry Letters* **2016,** 26, 3831-3837.
5. Gruden, G.; Barutta, F.; Kunos, G.; Pacher, P. Role of the endocannabinoid system in diabetes and diabetic complications. *British Journal of Pharmacology* **2016,** 173, 1116-1127.
6. Powell, D. R.; Gay, J. P.; Wilganowski, N.; Doree, D.; Savelieva, K. V.; Lanthorn, T. H.; Read, R.; Vogel, P.; Hansen, G. M.; Brommage, R.; Ding, Z. M.; Desai, U.; Zambrowicz, B. Diacylglycerol lipase a knockout mice demonstrate metabolic and behavioral phenotypes similar to those of cannabinoid receptor 1 knockout mice. *Frontiers in Endocrinology* **2015,** 6, 86-91.
7. Jung, K. M.; Clapper, J. R.; Fu, J.; D'Agostino, G.; Guijarro, A.; Thongkham, D.; Avanesian, A.; Astarita, G.; DiPatrizio, N. V.; Frontini, A.; Cinti, S.; Diano, S.; Piomelli, D. 2-arachidonoylglycerol signaling in forebrain regulates systemic energy metabolism. *Cell Metabolism* **2012,** 15, 299-310.
8. Ogasawara, D.; Deng, H.; Viader, A.; Baggelaar, M. P.; Breman, A.; den Dulk, H.; van den Nieuwendijk, A. M.; Soethoudt, M.; van der Wel, T.; Zhou, J.; Overkleeft, H. S.; Sanchez-Alavez, M.; Mo, S.; Nguyen, W.; Conti, B.; Liu, X.; Chen, Y.; Liu, Q. S.; Cravatt, B. F.; van der Stelt, M. Rapid and profound rewiring of brain lipid signaling networks by acute diacylglycerol lipase inhibition. *Proceedings of the National Academy of Sciences of the United States of America* **2016,** 113, 26-33.
9. Bisogno, T.; Howell, F.; Williams, G.; Minassi, A.; Cascio, M. G.; Ligresti, A.; Matias, I.; Schiano-Moriello, A.; Paul, P.; Williams, E. J.; Gangadharan, U.; Hobbs, C.; Di Marzo, V.; Doherty, P. Cloning of the first sn1-DAG lipases points to the spatial and temporal regulation of endocannabinoid signaling in the brain. *Journal of Cell Biology* **2003,** 163, 463-468.
10. Gao, Y.; Vasilyev, D. V.; Goncalves, M. B.; Howell, F. V.; Hobbs, C.; Reisenberg, M.; Shen, R.; Zhang, M. Y.; Strassle, B. W.; Lu, P.; Mark, L.; Piesla, M. J.; Deng, K.; Kouranova, E. V.; Ring, R. H.; Whiteside, G. T.; Bates, B.; Walsh, F. S.; Williams, G.; Pangalos, M. N.; Samad, T. A.; Doherty, P. Loss of retrograde endocannabinoid signaling and reduced adult

neurogenesis in diacylglycerol lipase knock-out mice. *The Journal of neuroscience : the official journal of the Society for Neuroscience* **2010,** 30, 2017-2024.

11. Tanimura, A.; Yamazaki, M.; Hashimotodani, Y.; Uchigashima, M.; Kawata, S.; Abe, M.; Kita, Y.; Hashimoto, K.; Shimizu, T.; Watanabe, M.; Sakimura, K.; Kano, M. The Endocannabinoid 2-arachidonoylglycerol produced by diacylglycerol lipase alpha mediates retrograde suppression of synaptic transmission. *Neuron* **2010,** 65, 320-327.
12. Shonesy, B. C.; Bluett, R. J.; Ramikie, T. S.; Baldi, R.; Hermanson, D. J.; Kingsley, P. J.; Marnett, L. J.; Winder, D. G.; Colbran, R. J.; Patel, S. Genetic Disruption of 2-Arachidonoylglycerol Synthesis Reveals a Key Role for Endocannabinoid Signaling in Anxiety Modulation. *Cell Reports* **2014,** 9, 1644-1653.
13. Cota, D. Role of the endocannabinoid system in energy balance regulation and obesity. *Frontiers of Hormone Research* **2008,** 36, 135-145.
14. Bermudez-Silva, F. J.; Cardinal, P.; Cota, D. The role of the endocannabinoid system in the neuroendocrine regulation of energy balance. *Journal of Psychopharmacology* **2012,** 26, 114-124.
15. Baggelaar, M. P.; Janssen, F. J.; van Esbroeck, A. C.; den Dulk, H.; Allara, M.; Hoogendoorn, S.; McGuire, R.; Florea, B. I.; Meeuwenoord, N.; van den Elst, H.; van der Marel, G. A.; Brouwer, J.; Di Marzo, V.; Overkleeft, H. S.; van der Stelt, M. Development of an activity-based probe and in silico design reveal highly selective inhibitors for diacylglycerol lipase-alpha in brain. *Angewandte Chemie International Edition* **2013,** 52, 12081-12085.
16. Baggelaar, M. P.; Chameau, P. J. P.; Kantae, V.; Hummel, J.; Hsu, K. L.; Janssen, F.; van der Wel, T.; Soethoudt, M.; Deng, H.; den Dulk, H.; Allara, M.; Florea, B. I.; Di Marzo, V.; Wadman, W. J.; Kruse, C. G.; Overkleeft, H. S.; Hankemeier, T.; Werkman, T. R.; Cravatt, B. F.; van der Stelt, M. Highly selective, reversible inhibitor identified by comparative chemoproteomics modulates diacylglycerol lipase activity in neurons. *Journal of the American Chemical Society* **2015,** 137, 8851-8857.
17. Hsu, K. L.; Tsuboi, K.; Adibekian, A.; Pugh, H.; Masuda, K.; Cravatt, B. F. DAGLbeta inhibition perturbs a lipid network involved in macrophage inflammatory responses. *Nature Chemical Biology* **2012,** 8, 999-1007.
18. Bisogno, T.; Howell, F.; Williams, G.; Minassi, A.; Cascio, M. G.; Ligresti, A.; Matias, I.; Schiano-Moriello, A.; Paul, P.; Williams, E. J.; Gangadharan, U.; Hobbs, C.; Di Marzo, V.; Doherty, P. Cloning of the first sn1-DAG lipases points to the spatial and temporal regulation of endocannabinoid signaling in the brain. *The Journal of Cell Biology* **2003,** 163, 463-468.
19. Baggelaar, M. P.; Janssen, F. J.; van Esbroeck, A. C. M.; den Dulk, H.; Allara, M.; Hoogendoorn, S.; McGuire, R.; Florea, B. I.; Meeuwenoord, N.; van den Elst, H.; van der Marel, G. A.; Brouwer, J.; Di Marzo, V.; Overkleeft, H. S.; van der Stelt, M. Development of an Activity-Based Probe and In Silico Design Reveal Highly Selective Inhibitors for Diacylglycerol Lipase-alpha in Brain. *Angewandte Chemie International Edition* **2013,** 52, 12081-12085.
20. Marrs, W. R.; Blankman, J. L.; Horne, E. A.; Thomazeau, A.; Lin, Y. H.; Coy, J.; Bodor, A. L.; Muccioli, G. G.; Hu, S. S. J.; Woodruff, G.; Fung, S.; Lafourcade, M.; Alexander, J. P.; Long, J. Z.; Li, W. W.; Xu, C.; Moller, T.; Mackie, K.; Manzoni, O. J.; Cravatt, B. F.; Stella,

N. The serine hydrolase ABHD6 controls the accumulation and efficacy of 2-AG at cannabinoid receptors. *Nature Neuroscience* **2010,** 13, 951-967.

21. Pribasnig, M. A.; Mrak, I.; Grabner, G. F.; Taschler, U.; Knittelfelder, O.; Scherz, B.; Eichmann, T. O.; Heier, C.; Grumet, L.; Kowaliuk, J.; Romauch, M.; Holler, S.; Anderl, F.; Wolinski, H.; Lass, A.; Breinbauer, R.; Marsche, G.; Brown, J. M.; Zimmermann, R. alpha/beta Hydrolase Domain-containing 6 (ABHD6) Degrades the late endosomal/lysosomal lipid bis(monoacylglycero)phosphate. *Journal of Biological Chemistry* **2015,** 290, 29869-29881.
22. Hosokawa, M. Structure and catalytic properties of carboxylesterase isozymes involved in metabolic activation of prodrugs. *Molecules* **2008,** 13, 412-431.
23. Speers, A. E.; Adam, G. C.; Cravatt, B. F. Activity-based protein profiling in vivo using a copper(I)-catalyzed azide-alkyne [3+2] cycloaddition. *Journal of the American Chemical Society* **2003,** 125, 4686-4687.
24. Liu, Y.; Patricelli, M. P.; Cravatt, B. F. Activity-based protein profiling: the serine hydrolases. *Proceedings of the National Academy of Sciences of the United States of America* **1999,** 96, 14694-14699.
25. Kidd, D.; Liu, Y.; Cravatt, B. F. Profiling serine hydrolase activities in complex proteomes. *Biochemistry* **2001,** 40, 4005-4015.
26. Patricelli, M. P.; Giang, D. K.; Stamp, L. M.; Burbaum, J. J. Direct visualization of serine hydrolase activities in complex proteomes using fluorescent active site-directed probes. *Proteomics* **2001,** 1, 1067-1071.
27. Hsu, K.-L. L.; Tsuboi, K.; Adibekian, A.; Pugh, H.; Masuda, K.; Cravatt, B. F. DAGLβ inhibition perturbs a lipid network involved in macrophage inflammatory responses. *Nature Chemical Biology* **2012,** 8, 999-1007.
28. Baggelaar, M. P.; Janssen, F. J.; van Esbroeck, A. C.; den Dulk, H.; Allarà, M.; Hoogendoorn, S.; McGuire, R.; Florea, B. I.; Meeuwenoord, N.; van den Elst, H.; van der Marel, G. A.; Brouwer, J.; Di Marzo, V.; Overkleeft, H. S.; van der Stelt, M. Development of an Activity-Based Probe and In Silico Design Reveal Highly Selective Inhibitors for Diacylglycerol Lipase-α in Brain. *Angewandte Chemie International Edition* **2013,** 52, 12081-12085.
29. Bachovchin, D. A.; Ji, T.; Li, W.; Simon, G. M.; Blankman, J. L.; Adibekian, A.; Hoover, H.; Niessen, S.; Cravatt, B. F. Superfamily-wide portrait of serine hydrolase inhibition achieved by library-versus-library screening. *Proceedings of the National Academy of Sciences of the United States of America* **2010,** 107, 20941-20946.
30. Alexander, J. P.; Cravatt, B. F. Mechanism of carbamate inactivation of FAAH: implications for the design of covalent inhibitors and in vivo functional probes for enzymes. *Chemistry & Biology* **2005,** 12, 1179-1187.